Hydrogen bonding and tunneling in the 2-pyridone·2-hydroxypyridine dimer. Effect of electronic excitation

ARTICLE *in* CHEMICAL PHYSICS · OCTOBER 2002

Impact Factor: 1.65 · DOI: 10.1016/S0301-0104(02)00598-0

ELSEVIER

Chemical Physics 283 (2002) 341–354

Chemical Physics

www.elsevier.com/locate/chemphys

Hydrogen bonding and tunneling in the 2-pyridone · 2-hydroxypyridine dimer. Effect of electronic excitation

David R. Borst[a], Joseph R. Roscioli[a], David W. Pratt[a,*], Gina M. Florio[b], Timothy S. Zwier[b], Andreas Müller[c], Samuel Leutwyler[c]

[a] *Department of Chemistry, University of Pittsburgh, 605 Chevron Science Center, Pittsburgh, PA 15260, USA*
[b] *Department of Chemistry, Purdue University, West Lafayette, IN 47907-1393, USA*
[c] *Departement für Chemie und Biochemie, Universitat Bern, Freiestrasse 3, CH-3000 Bern 9, Switzerland*

Received 21 March 2002

Abstract

The 2-pyridone · 2-hydroxypyridine (2PY · 2HP) mixed dimer has been studied using high resolution ultraviolet spectroscopy in the region of the 2PY S_1–S_0 origin, and fluorescence-dip infrared spectroscopy in the region of the hydride stretch fundamentals. The dense rotational structure of the electronic spectrum is characteristic of a *b*-type transition with a transition moment at $8° \pm 3°$ to the *b*-axis, consistent with excitation of the 2PY half of the dimer. A tunneling splitting of 520 ± 10 MHz appears in the spectrum, due to a double proton transfer in 2PY · 2HP. The double proton transfer exchanges the chemical identity of the two monomer units, thereby leading to a double tautomerization. Theoretical calculations suggest that the barrier to such motion is about 8 kcal/mol in the ground state; hence, the observed tautomerization apparently occurs in the excited state. An approximate fit of the high resolution spectrum gives rotational constants that are consistent with an excited state structure in which only the OH···O hydrogen bond in the dimer is lengthened substantially. The infrared spectrum out of the pair of ground state zero-point tunneling levels in the XH stretch region is reminiscent of that in the pure $(2PY)_2$ dimer. Its peak absorption frequency is at 2700 cm^{-1}, but the infrared band is spread over about 500 cm^{-1}, with reproducible sub-structure due to strong, anharmonic coupling. The excited state spectrum, in contrast, is dominated by a transition at 3135 cm^{-1}. This band is assigned to the OH fundamental, which is shifted to higher frequency by the weakening of the OH···O hydrogen bond upon electronic excitation.

1. Introduction

2-Pyridone (2PY) and 2-hydroxypyridine (2HP) are *keto–enol* tautomers of one another. This tautomeric pair has received much attention in the past largely because the two tautomers are very similar in energy, with both present in substantial

* Corresponding author. Tel.: +1-412-624-8660; fax: +1-412-624-8611.
E-mail addresses: pratt@pitt.edu (D.W. Pratt), zwier@purdue.edu (T.S. Zwier), samuel.leutwyler@iac.unibe.ch (S. Leutwyler).

0301-0104/02/$ - see front matter
PII: S0301-0104(02)00598-0

concentrations at room temperature, facilitating their study under a wide range of conditions [1–5]. The barrier to tautomerization is large in the monomers, because H-atom tunneling must occur over a large distance with substantial heavy atom rearrangement. Theoretical values of this barrier fall in the range of 35–38 kcal/mol [6].

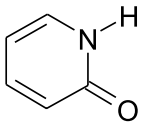

2-pyridone (2PY)

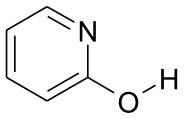

2-hydroxypyridine (2HP)

A substantial reduction in the barrier to tautomerization is predicted on complex formation [6]. The two tautomers have complementary H-bonding sites that are adjacent to one another; the NH donor and C=O acceptor sites in 2PY become pyridinal nitrogen acceptor and OH donor sites in 2HP. As a result, the tautomers can form stable complexes with many other species, including H_2O and NH_3 [1,4,5,7,8]. The two tautomers also can form three chemically distinct and strongly bound dimers; the $(2PY)_2$ and $(2HP)_2$ homodimers, and the $2PY \cdot 2HP$ mixed dimer [9–12].

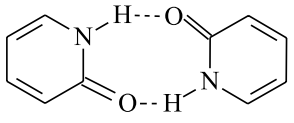

$(2PY)_2$

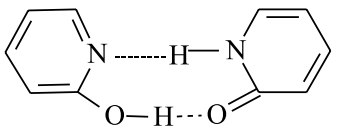

$2PY{\cdot}2HP$

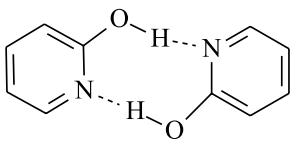

$(2HP)_2$

The recent calculations of Müller et al. [12] predict D_0 values for the $(2PY)_2$, $2PY \cdot 2HP$, and $(2HP)_2$ dimers of 17.6, 13.6, and 14.1 kcal/mol, respectively. In the symmetric dimers, tautomerization involves a double H-atom transfer in a distinctly asymmetric double well that interconverts the two dimers:

$$(2PY)_2 \rightleftharpoons (2HP)_2$$

As a result, no tunneling splitting is anticipated in these dimers. Indeed, the $(2PY)_2$ dimer, whose S_2–S_0 origin transition has been fully rotationally resolved and analyzed [9,10], exhibits no tunneling splitting.

The $2PY \cdot 2HP$ mixed dimer, which contains both the *keto* and *enol* tautomers, can undergo a double H-atom transfer that exchanges the two monomers' chemical identities in a symmetric double well:

$$2PY \cdot 2HP \rightleftharpoons 2HP \cdot 2PY$$

Here, a tunneling splitting is anticipated, and will reflect the rate of exchange between the two wells. Resolution of such tunneling splittings is anticipated to require high resolution spectroscopy, as recently demonstrated by Remmers et al. [13], who resolved a tunneling splitting for double H-atom transfer of ~1100 MHz (~0.04 cm^{-1}) in the benzoic acid dimer.

The mechanism of excited state double proton transfer after photoexcitation of canonical base pairs has attracted a great deal of experimental and theoretical interest. Given the close chemical similarity of 2PY to uracil and of 2HP to *iso*guanine, the rate of tunneling in dimers such as $2PY \cdot 2HP$ is of fundamental importance because of its implication in radiation induced mutations resulting from the formation of the rare *enol* tautomeric form of the nucleobases during DNA replication [14].

A second motivation for the present study is to probe the cooperatively strengthened hydrogen bonds in the $2PY \cdot 2HP$ dimer by comparison to those in the symmetric $(2PY)_2$ dimer. The infrared spectrum of $(2PY)_2$ in the hydride stretch region has recently been studied by Matsuda et al. [4]. It shows a broad, intense NH stretch absorption shifted down almost 700 cm^{-1} in frequency, as is

characteristic of strongly H-bonded dimers. In that case, the spectrum reflects the presence of two equivalent NH···O hydrogen bonds, which are strongly coupled to one another. We seek here to probe changes in the hydride stretch infrared spectrum induced by the somewhat weaker binding energy of the 2PY · 2HP dimer by comparison to $(2PY)_2$, and its inclusion of two different H-bonds (one NH···N and one OH···O).

Finally, by recording the hydride stretch infrared spectrum in the S_1 excited state, we will probe the effect of electronic excitation of the 2PY tautomer on H-bonding in the 2PY · 2HP dimer. This dimer is a model system in which to study the effects of electronic excitation on hydrogen bonding, because both tautomers, 2PY and 2HP, have accessible electronically excited states. The S_1 state of the 2PY monomer is about 5000 cm^{-1} below that of 2HP, so it is anticipated that electronic excitation will be localized on one or the other of the tautomers. The recent studies of Müller et al. [12] have identified transitions in the vicinity of the $(2PY)_2$ S_2–S_0 transition that they assign to the S_1–S_0 transition of the 2PY · 2HP dimer involving localized excitation of the 2PY tautomer in the dimer, $(2PY)^*$ · 2HP. That work concentrated on the vibronic spectroscopy of 2PY · 2HP and its deuterated isotopomers, with particular attention focused on intermolecular vibrations.

The present study builds on that work with two complementary experiments that shed new light on the effect of electronic excitation on the H-bonding and tunneling in the 2PY · 2HP dimer. A high resolution study of the 2PY · 2HP S_1–S_0 origin is used to identify tunneling splitting ascribable to the double proton transfer, and to measure the qualitative structural changes which accompany electronic excitation. Fluorescence-dip infrared spectra in the S_0 and S_1 states are then used to probe the effects of H-bonding on the hydride stretch vibrations in both states. We shall see that these data lead to a picture of the effects of electronic excitation which confirms and sharpens the deductions of Müller et al. [12], based on their vibronic spectroscopy. The primary effect of electronic excitation in the 2PY · 2HP dimer is to weaken, and thus elongate the OH···O hydrogen bond, while producing a much smaller effect on the NH···N hydrogen bond.

2. Experimental

Ultraviolet (UV) experiments with vibronic resolution were performed at both the University of Pittsburgh and Purdue University. The Pittsburgh apparatus has been described previously [15]. Briefly, the sample of 2HP was heated to 420 K, entrained in 5 bar of helium, and expanded into a vacuum chamber using a 1 mm diameter pulsed valve (General Valve Series 9) operating at 10 Hz. The expansion was crossed by the frequency doubled output of a dye laser (Quanta Ray PDL-1) operating with DCM and pumped by the second harmonic of a Nd^{3+}:YAG laser (Quanta Ray DCR-1A), also operating at 10 Hz. The resulting fluorescence was collected by a photomultiplier tube, processed by a boxcar integrator, and digitally recorded by a data acquisition computer.

The Purdue apparatus and methods have also been described previously [16]. In this case, the jet-cooled dimers were prepared by flowing a 70% neon/30% helium mixture at a backing pressure of 2–3 bar over a sample of 2HP heated to 370 K. The mixture was expanded from a pulsed valve (0.8 mm dia.) into a chamber pumped by a Roots blower. Fluorescence excitation spectra were recorded by crossing the expansion 5 mm downstream from the nozzle with the doubled output of a Nd^{3+}:YAG-pumped dye laser operating with DCM dye in methanol. Unfocused pulse energies of about 300 μJ/pulse were typically used. The fluorescence was collected by an f/1 lens and imaged onto a UV-enhanced photomultiplier tube.

Infrared (IR) spectra were recorded at Purdue using the fluorescence-dip infrared (FDIR) technique [16]. In this method, the fluorescence intensity of a selected transition in the excitation spectrum is monitored with an ultraviolet laser. Every other UV laser pulse was preceded by 150 ns with a counter-propagating, spatially overlapped IR pulse from an infrared parametric converter (LaserVision, 1–2 mJ/pulse, 0.25 cm^{-1} resolution). When the IR laser pulse is resonant with an infrared transition out of the level being monitored

in LIF, the population of that level is decreased. This decrease in population is detected as a dip in the UV fluorescence signal. The difference in the fluorescence signal obtained without and with the IR laser present is recorded as a function of IR frequency using the active baseline subtraction mode of a gated integrator, which is interfaced to a personal computer.

A similar technique was used to measure the IR spectrum of the electronically excited state. In this case, the IR pulse was delayed so as to occur during the lifetime of the excited state level probed by the UV laser. The S_1 origin lifetime of the 2PY · 2HP dimer was measured to be 14 ± 2 ns. When the IR light is resonant with a transition out of the S_1 zero-point level, it transfers population to vibrational levels 3100 cm^{-1} or more above the zero-point level. Fast non-radiative processes quench the fluorescence of these levels, leading to a dip in the fluorescence. Careful control of the time delay of the IR parametric converter from the UV laser (~20 ns in this case) was required in order to completely remove contributions to the spectrum from the ground state level, yet retain sufficient excited state population to record the S_1 FDIR spectrum with a good signal-to-noise ratio. A second gated integrator, gated on the rising edge of the fluorescence signal, was used to correct for shot-to-shot fluctuations in the fluorescence signal.

Finally, fluorescence excitation spectra at high resolution were obtained in Pittsburgh using the CW molecular beam spectrometer described in detail elsewhere [17]. The present conditions were as follows. The sample containing 2HP was heated to 450 K and entrained in 1–2 bar He. The mixture was expanded through a 280 μm quartz nozzle held at 470 K into a vacuum chamber. The resulting molecular beam was skimmed about 2 cm downstream of the nozzle before entering a second differentially pumped chamber where it was probed 10 cm downstream of the nozzle. The excitation source was an Ar^+ pumped CW single frequency tunable ring laser operating with DCM dye and frequency doubled by an intracavity $LiIO_3$ crystal. Typical powers used were 500 μW in the UV. The spectra were acquired at a rate of 50 Hz over a 2000 s scan. Four signals were collected. The PMT signal was collected with spatially selective optics using photon counting and stored on data acquisition computer. A signal from a near-confocal interferometer having a mode-matched free spectral range of 599.504 ± 0.005 MHz in the UV was collected to perform relative frequency calibration. The absorption spectrum of I_2 was collected to determine the absolute transition frequencies, which are accurate to ±3 MHz. Finally, the power signal was collected to normalize the PMT signal.

Supplementing the experimental work, we also performed density functional theory calculations using the BLYP/6-31+G* and B3LYP/6-311++G(d,p) methods [12,18]. Full geometry optimizations were carried out, followed by harmonic vibrational frequency calculations.

2-Hydroxypyridine (2HP) was commercially available (Aldrich) and used as received. Deuteration of the sample was accomplished by exchange with CH_3OD.

3. Results

Fig. 1 shows the low resolution fluorescence excitation spectrum of 2PY in the vicinity of the S_2–S_0 origin band of the 2PY dimer, $(2PY)_2$, which appears at 30 776 cm^{-1} [9,10]. Approximately 120 cm^{-1} to the red of this band, at 30 656 cm^{-1}, is a single band that has recently been identified by Müller et al. [12] as the S_1–S_0 origin band of the 2PY · 2HP dimer. When the experiment was repeated using a sample containing a 1:1 mixture of protonated and deuterated 2HP, three new bands appear in the vicinity of 30 656 cm^{-1}, one to the red and two to the blue. Using mass-resolved REMPI spectroscopy, Müller et al. [12] have assigned the band at 30 665 cm^{-1} to the doubly deuterated d_2(N–D/O–D) dimer and the bands at 30 681 and 30 640 cm^{-1} to the two partially deuterated d_1(N–D) and d_1(O–D) dimers. The latter two bands are resolved because the two positions of deuterium substitution are inequivalent in the mixed dimer, as we have confirmed in independent low resolution experiments. Furthermore, as Müller et al. [12] surmised, the close proximity of the 2PY · 2HP origin transition (30 656 cm^{-1}) to

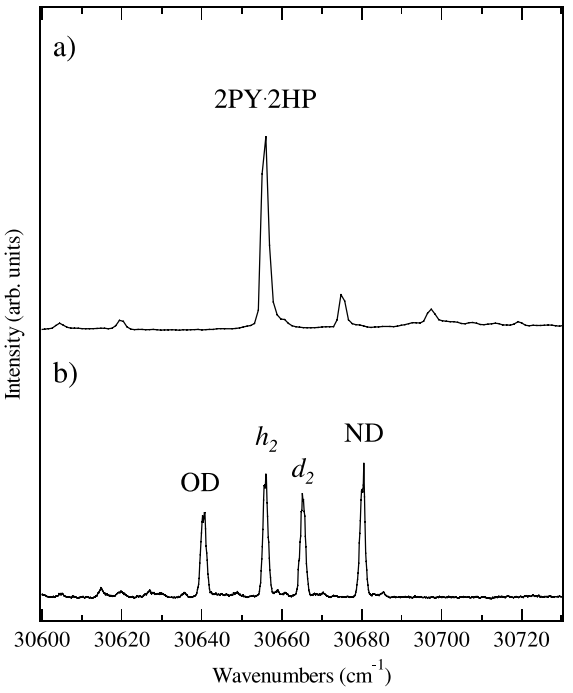

Fig. 1. Low resolution fluorescence excitation spectrum in the region of the 2PY · 2HP S_1–S_0 origin: (a) protonated sample; (b) spectrum obtained with a 1:1 H:D mixture in the labile N–H and O–H positions.

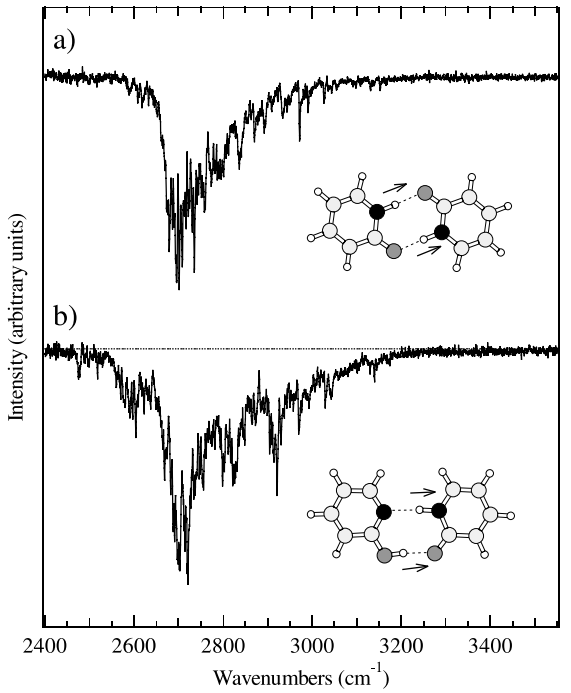

Fig. 2. Ground state fluorescence-dip infrared spectra of (a) $(2PY)_2$ and (b) 2PY · 2HP dimers in the hydride stretch region of the infrared.

that of the $h_2(2PY)_2$ (30 776 cm^{-1}) suggests that the electronic excitation is localized on the 2PY molecule in the mixed dimer. This was confirmed by the high resolution experiments (vide infra).

3.1. Ground state fluorescence-dip infrared spectra

Figs. 2(a) and (b) show the ground state IR spectra of the $(2PY)_2$ and 2PY · 2HP dimers in the hydride stretching region (2400–3550 cm^{-1}), respectively, as obtained by the FDIR technique. The spectrum of $(2PY)_2$ was obtained with the UV laser fixed at the S_2–S_0 origin (30 776 cm^{-1}) and is identical to that described previously by Matsuda et al. [4]. The spectrum is reproduced here for comparison with the corresponding spectrum of the 2PY · 2HP dimer shown below it. The latter spectrum was obtained with the UV laser fixed at the 2PY · 2HP S_1–S_0 origin (30 656 cm^{-1}). Besides the weak transitions above 3000 cm^{-1} (due to the aromatic CH stretch fundamentals), the entire absorption shown in Fig. 2 derives its oscillator strength from the XH stretch fundamentals involved in the strong H-bonds that hold the dimer together (NH/NH in $(2PY)_2$ and NH/OH in the 2PY · 2HP dimer).

Not surprisingly, several of the most obvious features of the spectrum of the 2PY · 2HP dimer (Fig. 2(b)) closely resemble those of the 2PY dimer above it (Fig. 2(a)). First, the spectrum is extremely broad, with absorption intensity spread over almost 500 cm^{-1}. Second, the band maximum of Fig. 2(b) occurs at about 2700 cm^{-1}, corresponding to frequency shifts of about 750 cm^{-1} from the NH stretch fundamental of the 2PY monomer (3448 cm^{-1}) and 900 cm^{-1} from the OH stretch fundamental of the 2HP monomer (3598 cm^{-1}). Third, the XH stretch band exhibits dense, reproducible sub-structure with an average spacing of some 5–10 cm^{-1}. Finally, the transition is unusually intense, with integrated absorption intensity that is easily a factor of 50 greater than that of either monomer's XH stretch fundamental.

All these shared features in the infrared spectra of Fig. 2 reflect the strong, cooperatively strengthened hydrogen bonds present in both dimers. In the $(2PY)_2$ dimer, a single NH stretch infrared fundamental carries the oscillator strength of the entire band. The two equivalent NH bonds are coupled to one another, forming NH stretch normal modes of a_g and b_u symmetry. In the former, the two NH bonds stretch in-phase with one another (i.e., both bonds stretch simultaneously) while in the latter, one NH bond stretches while the other contracts, as shown in the inset of Fig. 2(a). The b_u symmetry fundamental is IR allowed, while the lower frequency a_g mode is forbidden. The splitting between the b_u and a_g fundamentals is calculated to be 59 cm^{-1}. Matsuda et al. [4] observed the a_g fundamental at 2600 cm^{-1} in the Raman spectrum, about 100 cm^{-1} below the IR maximum in Fig. 2(a).

In contrast, in the 2PY · 2HP mixed dimer, the NH and OH groups are inequivalent, though they are still strongly coupled to one another. Thus, the calculated harmonic vibrational frequencies and infrared intensities for the mixed dimer show an intense band due to the out-of-phase oscillation of the two XH groups, but also show weak intensity in the lower frequency 'in- phase' band. A closer comparison of the spectra of Fig. 2(a) and (b) shows that there is a weak band on the low frequency side of the main band in the mixed dimer's spectrum at ~2600 cm^{-1} (Fig. 2(b)) that is not present in the 2PY dimer spectrum above it. We tentatively assign this sideband to the weakly allowed in-phase XH stretch fundamental.

The breadth and sub-structure of the spectrum results from the strong, anharmonic coupling of the XH stretch vibration(s) with background states that spreads the XH stretch oscillator strength over a host of bands spanning more than 500 cm^{-1}. Recent theoretical analyses of the IR spectra of benzoic acid [19] and formic acid dimers [20] indicates that, in these cases, the dominant anharmonic term is a 2:1 Fermi resonance of the XH stretch(es) with the overtones and combinations of the XH bend(s). However, there is no 'pure' XH bending vibration in these dimers. Some 15–20 combination bands spread over the 2500–3000 cm^{-1} region possess some degree of XH bend character, and thereby gain intensity through the 2:1 Fermi resonance. The large cubic anharmonic constant (~370 cm^{-1}) spreads the intensity over almost 500 cm^{-1}. Second tier couplings split the bands still further, leading to the observed, dense sub-structure. A similar behavior has been observed in other molecules containing H-bonded bridges across *cis*-amide groups [21].

3.2. Excited state fluorescence-dip infrared spectra

The S_2 state FDIR spectrum of $(2PY)_2$ and the S_1 state FDIR spectrum of the 2PY · 2HP dimer are shown in Fig. 3(a) and (b), respectively. The two spectra are very different from each other, and from the corresponding ground state spectra. That for the 2PY dimer was recorded with the UV pulse (at 30 776 cm^{-1}) preceding the IR pulse by 19 ns and is similar in appearance to that reported by

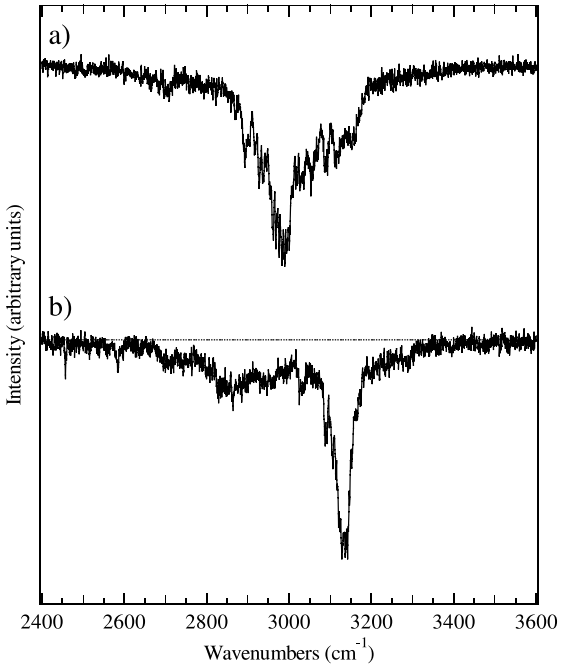

Fig. 3. Fluorescence-dip infrared spectra of the electronically excited dimers: (a) spectrum of $(2PY)_2$ recorded while monitoring fluorescence from its S_2 electronic origin at 30 776 cm^{-1}; (b) spectrum of 2PY · 2HP recorded while monitoring fluorescence from its S_1 electronic origin at 30 656 cm^{-1}. The delay between UV excitation laser and IR depletion laser is 19 ns in (a) and 24 ns in (b).

Matsuda et al. [4]. In the excited state spectrum, the XH stretch absorption maximum is shifted to higher frequency by $\sim$260 cm^{-1} relative to the ground state maximum at $\sim$2700 cm^{-1}. At the same time, the width of the band decreases from more than 500 cm^{-1} in S_0 to less than 300 cm^{-1} in S_2.

The corresponding spectrum of the S_1 state 2PY · 2HP dimer, recorded with the UV pulse preceding the IR by 24 ns, shows an even larger change upon electronic excitation. The dominant peak in the spectrum is shifted about 440 cm^{-1} to higher frequency in the excited state (3135 cm^{-1}) than it is in the ground state (2700 cm^{-1}). At the same time, the band sharpens still further to only 40 cm^{-1} full width at half maximum. Both these features point to a substantial weakening of one or both hydrogen bonds upon electronic excitation. A further interpretation of the spectrum of Fig. 3(b) will be taken up after the high resolution spectrum of the mixed dimer has been considered.

3.3. High resolution electronic spectroscopy of the S_1–S_0 origin

Fig. 4 shows the S_1–S_0 fluorescence excitation spectrum of the mixed (2PY · 2HP) dimer band (at 30 656 cm^{-1}) at high resolution. The band spans $\sim$3 cm^{-1} and contains thousands of lines, each exhibiting widths of order 100 MHz or less. (The homogeneous width expected from the measured fluorescence lifetime is $\sim$12 MHz.) The severe congestion of the spectrum has so far precluded a conventional fit. Individual lines have not been assigned to unique transitions between lower and upper state rovibronic levels because they could not be identified. However, valuable information has been extracted from an approximate analysis of the spectrum.

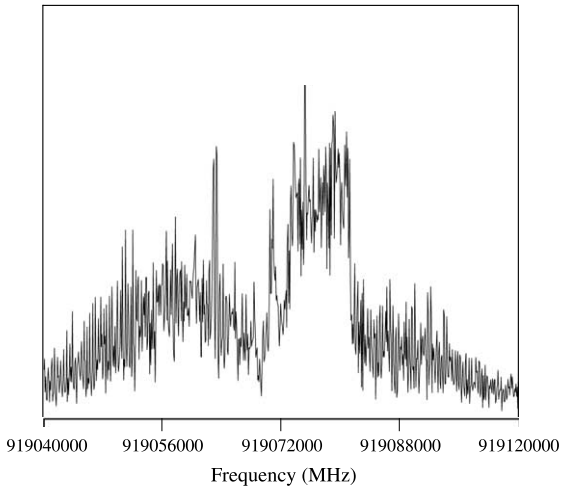

Fig. 4. High resolution fluorescence excitation spectrum of the 2PY · 2HP dimer at its S_1–S_0 origin (30 656 cm^{-1}).

The spectrum in Fig. 4 exhibits primarily *b*-type transitions. It also exhibits a small amount of *a*-type character in the strong, central Q-branch region of the spectrum. The relative intensities of these two types of transitions give an estimate of the angle between the optical transition moment and the *b* inertial axis of $\theta_{TM} = 8° \pm 3°$. Now, the S_1–S_0 TM in 2PY itself makes an angle of $-51°$ with respect to its *a*-axis [2]. The corresponding TM in 2HP makes an angle of $\pm 60°$ with respect to its *a*-axis [22]. If the S_1–S_0 excitation in the mixed 2PY · 2HP dimer is largely localized on the 2PY fragment, as we anticipate from the close proximity of the band to the S_1–S_0 origin of 2PY monomer, then we would expect its TM to lie near the dimer *b*-axis, as observed. This observation provides independent confirmation of the assignment of this band to the 2PY · 2HP mixed dimer.

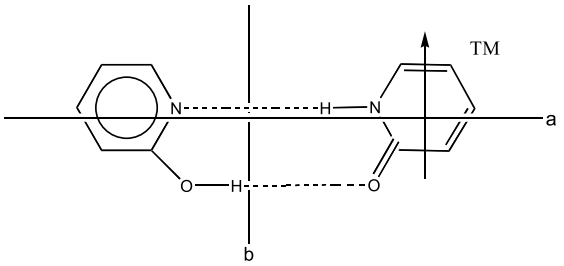

An approximate fit of the spectrum in Fig. 4 was obtained using a procedure developed by Remmers et al. [13] in their analysis of the incompletely resolved electronic spectrum of the benzoic acid dimer. First, theoretical values of rotational constants of the ground state of the 2PY · 2HP dimer were calculated using DFT methods (vide infra). These are listed in Table 1. Then, a simulated spectrum was generated using

Table 1
Approximate rotational constants (in MHz) of the 2PY · 2HP dimer of 2-hydroxypyridine in its S_0 and S_1 electronic states, compared to Hartree–Fock and density functional theoretical values

State	*A*	*B*	*C*
S_0 (exp.)	1707(15)[a]	327(5)	274(5)
S_0: SCF/6-31G(d,p)	[1713.35]	[328.55]	[275.68]
S_0: B3LYP/6-311++G(d,p)	[1671.09]	[341.66]	[283.66]
S_1 (exp.)[b]	1662(5)	327(3)	274(3)
S_1: CIS/6-31G(d,p)	[1718.66]	[322.31]	[271.61]
S_1–S_0	−45(5)	0(3)	0(3)
CIS–SCF	[+5.3]	[−6.2]	[−4.1]

[a] Uncertainties in parentheses.
[b] Origin at 30657.08(2) cm^{-1}.

the determined value of θ_{TM}, assuming identical constants for the S_1 state. Next, these constants were adjusted to provide the best match with the overall appearance of the experimental spectrum, using derivatives calculated with the aid of the Hellman–Feynman theorem. Finally, the ground state constants were adjusted, while keeping the differences in these constants between the two states fixed, in order to determine an approximate range of values for which a reasonable match to the spectrum could be made. These results are also listed in Table 1.

Finally, a further examination of the spectrum in Fig. 4 revealed that all of the stronger transitions are accompanied by a second transition at regular intervals. This suggests that the 2PY · 2HP dimer band at 30 656 cm^{-1} consists of two sub-bands. An autocorrelation analysis [23] was performed to measure the separation of the two sub-bands. This analysis is shown in Fig. 5. The distinct features on either side of the maximum at the origin indicate that two sub-spectra are present in Fig. 4, displaced by 520 ± 10 MHz. As will be seen, this splitting has its origin in a tunneling motion, in either the ground state or the excited state of 2PY · 2HP. A potential candidate for the tunneling motion is the double proton transfer associated with the 2PY · 2HP ⇌ 2HP · 2PY tautomerization.

3.4. Calculated structure of 2PY · 2HP in the ground state

The DFT B3LYP/6-311++G(d,p) calculations predict a ground state structure for the 2PY · 2HP dimer that is planar, with rotational constants that

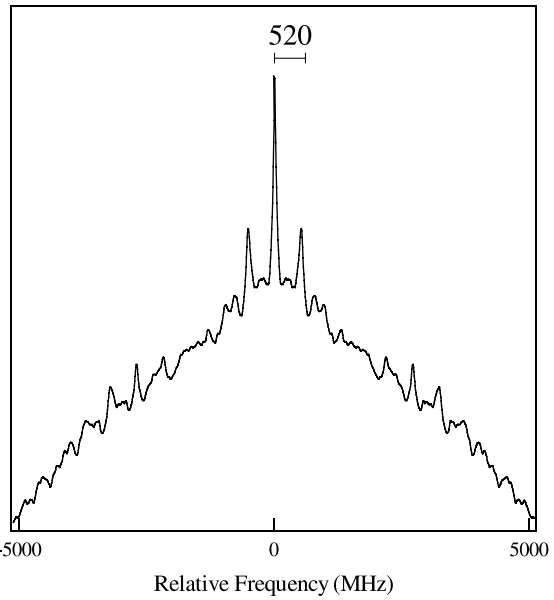

Fig. 5. Autocorrelation spectrum of the band in Fig. 4. The side bands at ±520 MHz indicate the presence of two bands in the spectrum, split by 520 MHz.

are in good agreement with experiment (cf. Table 1). According to theory, the 2PY · 2HP dimer has heavy atom separations of 2.646 Å (OH · · · O) and 2.915 Å (NH · · · N). The corresponding NH · · · O separations in the $(2PY)_2$ dimer are 2.78 Å, in very good agreement with the experimental value of 2.77 ± 0.03 Å [10]. Thus, the principal difference between the structures of the 2PY · 2HP and $(2PY)_2$ dimers is that the OH · · · O and NH · · · N bonds in 2PY · 2HP are about 0.12 Å shorter and 0.15 Å longer, respectively, than the NH · · · O bonds in $(2PY)_2$.

4. Discussion

The experimental data presented in the previous section provide two complementary views of the effect of electronic excitation on the hydrogen bonding and tunneling in the 2PY · 2HP mixed dimer. The high resolution spectrum of the S_1–S_0 origin transition provides new information about the structural changes that accompany electronic excitation and the hydrogen atom tunneling process. On the other hand, the S_0 and S_1 state FDIR data probe the hydrogen bonding in the two states via the response of the hydride stretch vibrations to electronic excitation.

The most obvious effect of electronic excitation is a decrease in the binding energy of the dimer. The 0_0^0 band of the S_1–S_0 transition of 2PY · 2HP is blue-shifted by 825 cm^{-1} from the "A" 0_0^0 band of the 2PY monomer at 29831 cm^{-1} [1,2]. This amounts to a decrease in binding energy of 2.36 kcal/mol upon electronic excitation. Müller et al. [12] have carried out DFT B3LYP calculations which predicts a ground state binding energy of 13.6 kcal/mol. Thus electronic excitation weakens the total binding of the dimer by about 20%, but how this decrease is distributed between the NH···N and OH···O hydrogen bonds that hold the dimer together is not clear from the electronic frequency shift alone.

More information about the structure of the 2PY · 2HP dimer in its S_1 state is provided by the change in its rotational constants upon electronic excitation. The A rotational constant decreases by ~45 MHz in going from S_0 to S_1, whereas the B and C rotational constants remain approximately the same (cf. Table 1). As shown in the structure below,

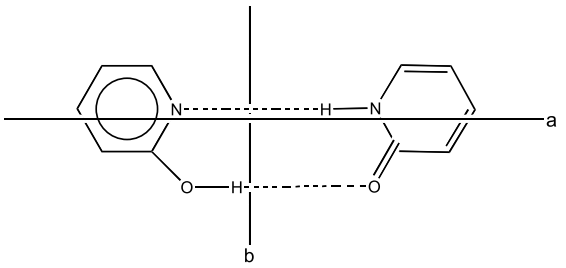

the B rotational constant is most sensitive to mass displacements along the line joining the centers-of-mass of the two monomers, whereas the A rotational constant is most sensitive to displacements perpendicular to this axis. The observed photoinduced changes in rotational constants thus suggest that, while there is little change in the radial separation of the two centers-of-mass, there is a displacement of one unit with respect to the other along an in-plane angular coordinate.

More specific information about the magnitudes of these effects can be obtained in the following way. Suppose we attribute the observed changes in the rotational constants to changes in only the intermolecular bond distances, ignoring possible changes in the geometries of the monomer units themselves. This leads to estimated heavy atom separations of 3.073 Å for the OH···O hydrogen bond and 3.081 Å for the NH···N hydrogen bond in the S_1 state. Comparing these distances to the theoretical values for the ground state, we see that the OH···O hydrogen bond length increases by ~0.3 Å when the photon is absorbed, whereas the NH···N hydrogen bond length increases by only ~0.1 Å. The two bonds weaken on electronic excitation. But the decrease in the OH···O bond strength is substantially larger than the decrease in the NH···N bond strength, thereby accounting for the angular displacement of one unit with respect to the other.

This model quite evidently overestimates the magnitude of the geometry change in the OH···O hydrogen bond. Nevertheless, its qualitative prediction is in excellent agreement with the calculations and the vibronic spectroscopy of Müller et al. [12]. These authors have carried out CIS calculations on the mixed dimer which predict an increase in the OH···O heavy atom separation of 0.06 Å, but a negligible (0.01 Å) change in the NH···N separation on S_1 excitation.

The asymmetric motion of the two monomers upon electronic excitation, in which the OH···O hydrogen bond lengthens while the NH···N hydrogen bond does not, would seem most closely related to the ν_3 'cogwheel' or 'opening' intermolecular vibration, calculated at 87 cm^{-1} [12].

However, the vibronic spectrum shows a dominant Franck–Condon progression in a mode with 158 cm^{-1} frequency, assigned by Müller et al. [12] to the intermolecular stretch, v_6, with a calculated value of 156 cm^{-1}. At the same time, there is no evidence for a progression in the cogwheel mode v_3. Fig. 6 shows the form of the 'cogwheel' and 'intermolecular stretch' normal modes from the DFT B3LYP calculation. Close inspection of these normal modes reveals that they are both mixtures of stretch and cogwheel motions, as noted by Müller et al. [12]. Furthermore, the OH···O separation is changed substantially by the intermolecular stretch motion, but hardly at all by the cogwheel mode. Thus, the nature of the geometry change deduced from the rotational analysis is at least qualitatively consistent with the Franck–Condon analysis based on the intermolecular motions from Müller et al. [12].

4.1. Changes in H-bonding from the infrared spectra

These structural deductions provide a foundation for a proper interpretation of the S_1 state FDIR spectrum. Fig. 7 makes a direct comparison between the ground state and excited state infrared spectra of 2PY · 2HP.

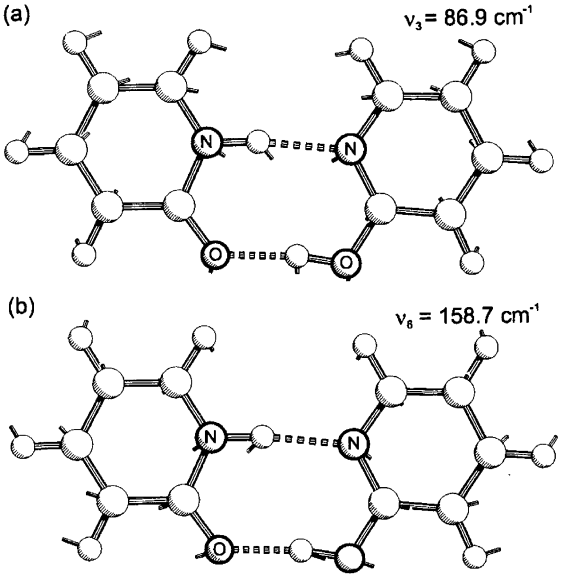

Fig. 6. Intermolecular normal mode eigenvectors for the v_3 'cogwheel' and v_6 'intermolecular stretch' vibrations, taken from the DFT B3LYP/6-311++G(d,p) calculation.

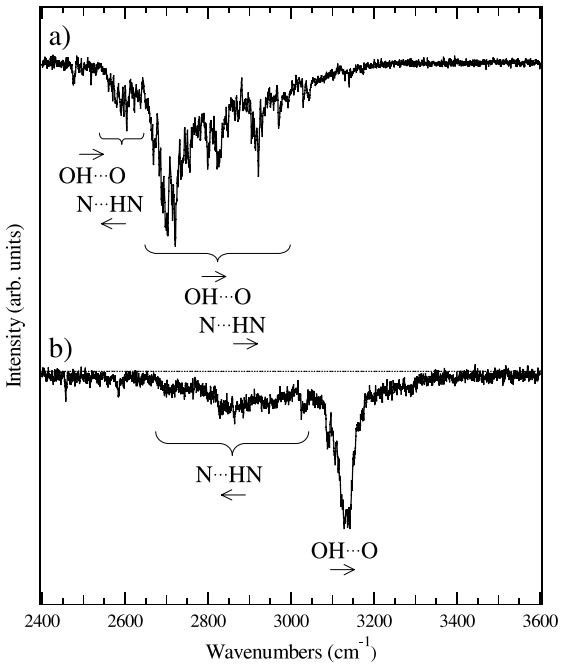

Fig. 7. A direct comparison of the (a) S_0 and (b) S_1 state FDIR spectra of the 2PY · 2HP dimer. Note the dramatic shift of the intense absorption to higher frequency in the electronically excited state. Proposed assignments are given on the absorptions.

In the ground electronic state, the OH···O and NH···N hydrogen bonds are both strong, and the OH and NH oscillations are strongly coupled to one another, as shown schematically in Fig. 7(a). The higher frequency mode is similar to the corresponding b_u symmetry fundamental in $(2PY)_2$, shown in Fig. 2(a), and carries most of the oscillator strength of the entire band. The lower frequency band, which correlates with the a_g symmetry fundamental in $(2PY)_2$, gains some oscillator strength due to the asymmetry of the 2PY · 2HP mixed dimer, producing the weak band near 2600 cm^{-1}.

In the S_1 state (Fig. 7(b)), the weakening of the OH···O hydrogen bond leads to a reduced coupling between the OH and NH bonds, making them more nearly local OH and NH stretches. The lengthening of the OH···O hydrogen bond upon electronic excitation then leads to an assignment of

the intense band near 3140 cm^{-1} to the OH stretch of the OH···O group, while the broad, less intense absorption over the 2800–3000 cm^{-1} region is assigned to the NH stretch of the NH···N group. If we estimate the frequencies of the uncoupled NH and OH groups in the ground state to be 2650 cm^{-1} (the average of the two observed frequencies at 2600 and 2700 cm^{-1}), then the S_1 state OH stretch is shifted to higher frequency by almost 500 cm^{-1}, while the NH stretch is also weakened, but by a much smaller amount ($\sim$250 cm^{-1}).

In point of fact, we do not know quantitatively the extent to which the coupling between OH and NH stretches is reduced by electronic excitation. However, the proposed assignment of the S_1 spectrum in terms of local mode NH and OH oscillators is consistent with a similar assignment of the S_1 state hydride stretch infrared spectrum of $2PY \cdot (H_2O)_1$ and $2PY \cdot (H_2O)_2$ by Matsuda et al. [4] and Zwier [24]. There, too, it is the OH···O hydrogen bond that appears to be weakened by the electronic excitation, while the NH···O hydrogen bond is hardly changed in frequency upon electronic excitation.

Additional insight into the origin of these effects is provided by theory. As noted, excitation of 2PY · 2HP by light is largely confined to the 2PY "side" of the dimer. Therefore, it is appropriate to consider the MO's of 2PY itself when thinking about the nature of the S_1–S_0 electronic transition in the 2PY · 2HP dimer. CIS calculations [18] show that the S_1–S_0 transition of 2PY consists mainly of a HOMO to LUMO excitation, leading to (a) a partial reversal of the bond order alternation in the ring, (b) an increase in electron density in the N–H bond, and (c) a decrease in electron density in the C=O bond. A reduced electron density in the C=O bond will, by simple electrostatic arguments, make it less attractive to the hydrogen atom of the OH group, reducing the strength of the OH···O bond. In agreement with this, our SCF/CIS calculations show that the structure of the 2HP side of the dimer is largely unaffected by S_1 excitation, except for a noticeable shortening of the OH bond. In contrast, the 2PY side of the dimer undergoes several structural changes, including changes in the ring bond lengths as large as 0.08 Å. Other calculations [25] support this view.

4.2. Tunneling

Having deduced the nature of the structural change accompanying electronic excitation, and the effect that this structural change has on the hydrogen bonding in the dimer, we return once again to the issue of the tunneling splitting observed in the electronic spectrum. The 2PY · 2HP mixed dimer can undergo a double proton transfer in which the tautomeric state of the two monomers is interchanged. This results in a symmetric double minimum potential well and associated tunneling splitting in each electronic state. Unfortunately, the experimentally measured tunneling splitting supplies only the *difference* in tunneling splittings between ground and excited states, not the absolute magnitude of the tunneling splitting in either state.

In order to gain further insight to the anticipated magnitude of the tunneling splitting in the ground electronic state, ab initio calculations were carried out to determine the barrier height and structural changes associated with the ground state double proton transfer process. The doubly hydrogen bonded equilibrium structure (ground state = GS) was optimized at the Hartree–Fock/6-31G(d,p) level, and with the hybrid B3LYP DFT method using the 6-311++G(d,p) valence triple zeta basis set. With both methods, GS is planar (C_s symmetric), in agreement with experiment; the B3LYP GS structure is shown in Fig. 8(a). The SCF rotational constants are in excellent agreement with experiment, while those predicted by the B3LYP/6-311++G(d,p) method are slightly smaller for A and larger for B, C (cf. Table 1).

The suitability of different quantum chemical methods for calculating proton transfer potentials and surfaces has been widely discussed. Current evidence is that the HF method overestimates proton transfer barriers and that correlated methods such as MP2 or coupled cluster methods are necessary to obtain very accurate barriers [26,27]. Relaxed MP2 calculations with large enough basis sets are prohibitive for a system with 14 second-row atoms. B3LYP calculations yield bar-

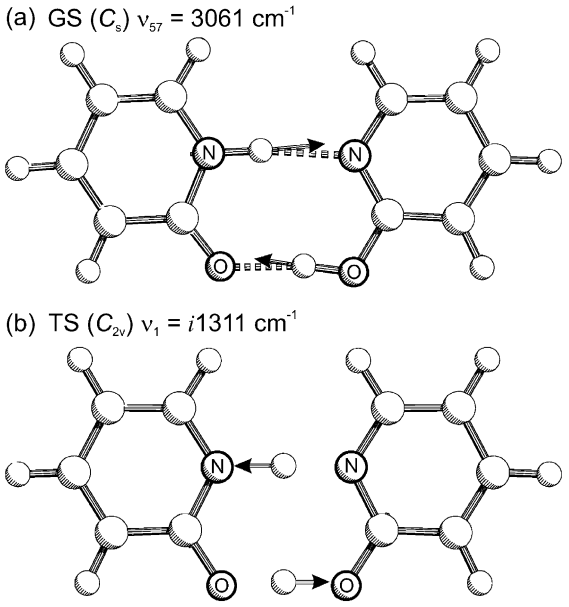

Fig. 8. B3LYP/6-311++G(d,p) calculated: (a) equilibrium structure (GS) with the vibrational eigenvector of the $\nu_{57} = 3061$ cm^{-1} normal mode, which correlates most closely with a pure double proton transfer motion, and (b) transition structure (TS) for double proton transfer with the eigenvector corresponding to the imaginary frequency i1311 cm^{-1}.

riers of 60–80% of the MP2 barrier height with a substantially smaller computational effort [26–28]. Hence, we also used B3LYP/6-311++G(d,p) for the calculation of the double proton transfer transition state (= TS). We first displaced the 2PY N–H proton in steps of 0.05 Å towards the 2HP moiety, fully optimizing the 2PY · 2HP geometry at each step. This leads to an asymmetric potential energy curve, since for large N–H distances the 2HP moiety is 'pushed away' from 2PY. The structure at the highest point of this PE curve was then further optimized to an index-1 saddle point by the QST2 procedure [18]. The TS structure is predicted to be planar and C_{2v} symmetric, as shown in Fig. 8(b). The finding of a single transition state for double proton transfer implies that the ground state proton transfer is *cooperative* .

During the proton transfer, both H bonds shorten considerably. The NH $\cdots$ N distance decreases by 0.33 Å from 2.91 to 2.58 Å and the OH $\cdots$ O distance decreases by 0.24 Å from 2.65 to 2.40 Å. Simultaneously, the N–H bond length increases from 1.04 to 1.29 Å and the O–H bond length increases from 1.00 to 1.20 Å.

The purely electronic barrier height, derived from the difference of B3LYP total energies, is 8.334 kcal/mol (2915 cm^{-1}). More relevant is the *vibrationally adiabatic* barrier height, for which the zero-point vibrational energies of all normal modes except the double proton transfer mode are added to the electronic barrier height. For the TS, this mode is the single mode with imaginary frequency, i1311 cm^{-1}, shown in Fig. 8(b). For the GS, the choice of the double proton transfer mode as $\nu_{57} = 3061$ cm^{-1} was unequivocal, since this is the N–H/O–H stretching mode which is most similar to the TS proton transfer mode, as shown in Fig. 8(b). The other two N–H/O–H stretching modes (ν_{58} and ν_{59}) involve much smaller N–H/O–H and larger C–H displacements. The resulting vibrationally adiabatic barrier is 7.666 kcal/mol (2681 cm^{-1}).

The double proton transfer path length was calculated by first superimposing the centers of mass of the GS and TS structures and then minimizing the relative distances of the corresponding atoms of 2HP and 2PY in the GS and TS structures. The distance between GS and TS

$$R(\mathrm{TS}-\mathrm{GS}) = \left\{ \sum_{i=1}^{24} m_i \Delta r_i^2 (\mathrm{TS}-\mathrm{GS}) \right\}^{1/2}$$

was calculated in mass-weighted Cartesian coordinates. Each individual distance, $\Delta r_i(\mathrm{TS}-\mathrm{GS})$ was approximated as a straight line, leading to a lower limit for the total mass-weighted distance, $R(\mathrm{TS}-\mathrm{GS}) = 2.21$ u$^{1/2}$Å. It should be realized that the length of this path is determined by the motions of the 2HP and 2PY frames, since each C, N and O atom moves 0.2 to 0.35 Å during the double proton transfer, see above.

The resulting symmetric double minimum potential for the S_0 state is shown in Fig. 9. The one-dimensional vibrational wave functions were calculated using a fourth-order Runge–Kutta method and are numerically precise to $\ll 10^{-6}$ cm^{-1} (30 kHz). The calculated splitting between the symmetric and antisymmetric $0^+/0^-$ vibrational ground states is $<10^{-6}$ cm^{-1}, much smaller than the observed splitting of 0.017 cm^{-1}.

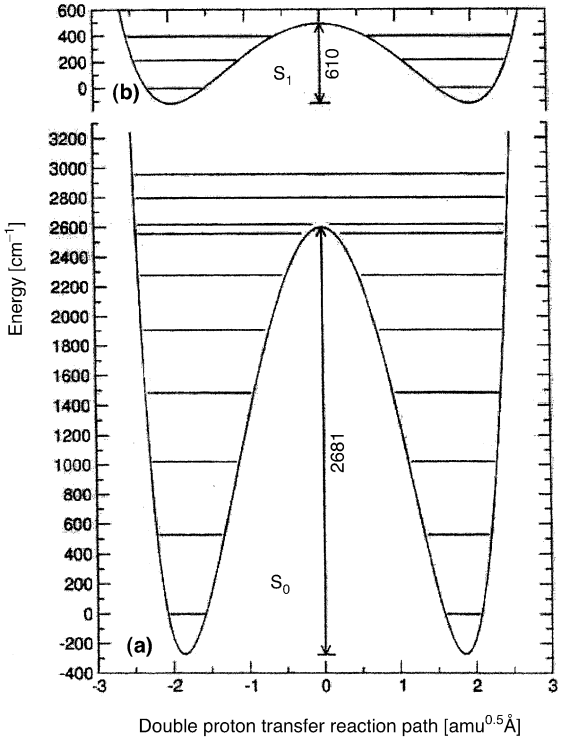

Fig. 9. Calculated model potential for double proton transfer in the ground and electronically excited states of the 2PY · 2HP dimer. (a) The barrier height in the ground state is the vibrationally adiabatic barrier of 2681 cm^{-1} calculated from the electronic and vibrational zero-point energies of GS and TS. The distance from GS to TS is in mass-weighted Cartesian coordinates. Tunneling splittings for $v = 0$–5 are not visible on the scale of the figure. (b) The excited state double proton transfer potential was constructed by arbitrarily assuming the same $R(\mathrm{TS} - \mathrm{GS})$ distance as for the S_0 state; the barrier was lowered to 610 cm^{-1} so as to yield the observed tunneling splitting of 520 MHz (0.0173 cm^{-1}), also not visible in the figure.

A higher level electronic calculation (MP2) would probably raise the barrier by an estimated 20–40%. A more quantitative evaluation of the double proton transfer path length $R(\mathrm{TS} - \mathrm{GS})$ in curvilinear coordinates and including counter-rotations of the 2HP and 2PY sub-units would increase the distance between GS and TS even further. It follows that the model potential in Fig. 9(a) leads to an *upper limit* for the tunneling splitting. We conclude that, if the observed tunneling splitting arises from the double proton transfer reaction, it must be due to tunneling in the S_1 excited state rather than the ground electronic state.

How much lower must the S_1 state barrier be to yield the observed tunneling splitting? For simplicity, we fixed $R(\mathrm{TS} - \mathrm{GS})$ at the S_0 state value, although it must increase, as the rotational analysis (vide supra) and the Franck–Condon analysis [14] have shown. Simple scaling of the barrier height to 610 cm^{-1} (1.74 kcal/mol) yielded the observed 520 MHz splitting. The resulting potential and the lowest three pairs of vibrations are shown in Fig. 9(b).

Before leaving the issue of tunneling, an alternative source of the tunneling splitting should be briefly considered. The CIS calculations of Müller et al. [12] predict that the 2PY monomer in the mixed dimer is slightly non-planar (pyramidal) about the N atom, with a 10 cm^{-1} barrier for interconversion between the two pyramidal structure. This gives rise to a double minimum potential well for interconversion between the two equivalent non-planar minima, with a tunneling splitting between 0^+ and 0^- levels. However, the ground state dimer is planar, with a zero-point level which is symmetric about the planar configuration (0^+). Transitions from this level will be only to the 0^+ excited state level, and cannot explain the tunneling splitting observed.

5. Conclusions

Combined data from high resolution electronic spectroscopy and S_0 and S_1 state infrared spectroscopy experiments have led to a more complete picture of the changes in hydrogen bonding that accompany electronic excitation in the mixed 2PY · 2HP dimer. The dominant change involves a significant weakening of the OH···O hydrogen bond in S_1 compared to S_0, perhaps accompanied by a smaller weakening of the NH···N hydrogen bond. That the former bond strength, rather than the latter, is principally affected by the absorption of a photon may be traced to the localization of the optical excitation on the 2PY side of the molecule.

The 2PY · 2HP dimer has also been shown to be a paradigm system for photoinduced double pro-

ton transfer in DNA base pairs. In the ground state, the double proton transfer, leading to cooperative tautomerization, is calculated to occur on a relaxed potential having a relatively high barrier of ≈8 kcal/mol, leading to a predicted tunneling splitting of $<10^{-6}$ cm^{-1}. Given the calculated ground state structure and the changes between the S_0 and S_1 states that can be inferred from experiment, the observed tunneling splitting of 520 ± 10 MHz can only be interpreted as a cooperative double proton transfer if the S_1 state has the relatively low barrier for double transfer of ≈1 kcal/mol. Such a tunneling process is intriguing because it involves both nuclear motion and simultaneous hopping of the electronic excitation between the two molecules. High resolution scans of deuterated isotopomers ultimately will be needed to probe the excited state tunneling in greater detail. Such scans are currently being pursued.

Acknowledgements

G.M.F. wishes to thank her Pittsburgh hosts for their hospitality during her research visit. This work has been supported by NSF (CHE-9728636 and CHE-9987048) and the Schweiz. Nationalfonds (Project 2000-61890).

References

[1] M.R. Nimlos, D.F. Kelley, E.R. Bernstein, J. Chem. Phys. 93 (1989) 643.
[2] A. Held, B.B. Champagne, D.W. Pratt, J. Chem. Phys. 95 (1991) 8372.
[3] L.D. Hatherly, R.D. Brown, P.D. Godfrey, A.P. Pierlot, W. Caminati, D. Damiani, S. Melandri, L.B. Favero, J. Chem. Phys. 97 (1993) 46.
[4] Y. Matsuda, T. Ebata, N. Mikami, J. Chem. Phys. 110 (1999) 8397.
[5] G.M. Florio, C.J. Gruenloh, R.C. Quimpo, T.S. Zwier, J. Chem. Phys. 113 (2000) 11143.
[6] V. Barone, C. Adamo, J. Chem. Phys. 99 (1995) 15062.
[7] A. Held, D.W. Pratt, J. Am. Chem. Soc. 115 (1993) 9708.
[8] A. Held, D.W. Pratt, J. Am. Chem. Soc. 115 (1993) 9718.
[9] A. Held, D.W. Pratt, J. Am. Chem. Soc. 112 (1990) 8629.
[10] A. Held, D.W. Pratt, J. Chem. Phys. 96 (1992) 4869.
[11] A. Müller, F. Talbot, S. Leutwyler, J. Chem. Phys. 112 (2000) 3717.
[12] A. Müller, F. Talbot, S. Leutwyler, J. Chem. Phys. 115 (2001) 5192.
[13] K. Remmers, W.L. Meerts, I. Ozier, J. Chem. Phys. 112 (2000) 10890.
[14] L. Stryer, in: Biochemistry, fourth ed., W.H. Freeman & Co, New York, 1995, p. 809.
[15] J.R. Johnson, K.D. Jordan, D.F. Plusquellic, D.W. Pratt, J. Chem. Phys 93 (1990) 2258.
[16] T.S. Zwier, Annu. Rev. Phys. Chem . 47 (1996) 205.
[17] W.A. Majewski, J.F. Pfanstiel, D.F. Plusquellic, D.W. Pratt, in: A.B. Myers, T.R. Rizzo (Eds.), Laser Techniques in Chemistry, Wiley, New York, 1995, p. 101.
[18] M.J. Frisch et al., Gaussian 98 (Revision A.7), Gaussian Inc, Pittsburgh, PA, 1998.
[19] G.M. Florio, E.L. Sibert III, T.S. Zwier, Faraday Discuss. 118 (2001) 315.
[20] E.L. Sibert III, K.D. Jordan, G.M. Florio, T.S. Zwier, in preparation.
[21] J.R. Carney, A.V. Fedorov, J.R. Cable, T.S. Zwier, J. Phys. Chem. A 105 (2001) 3487.
[22] D.R. Borst, J.R. Roscioli, D.W. Pratt, J. Phys. Chem. A 106 (2002) 4022.
[23] R.M. Helm, H.-P. Vogel, H.J. Neusser, Chem. Phys. Lett. 270 (1997) 285.
[24] T.S. Zwier, J. Phys. Chem. 105A (2001) 8827.
[25] P.-T. Chou, C.-Y. Wei, F.-T. Hung, J. Phys. Chem. 101B (1997) 9119.
[26] S. Sadukhan, D. Munoz, C. Adamo, G.E. Scuseria, Chem. Phys. Lett. 306 (1999) 83.
[27] M. Meuwly, A. Bach, S. Leutwyler, J. Am. Chem. Soc. 123 (2001) 11446.
[28] T. Loerting, K.R. Liedl, B.M. Rode, J. Chem. Phys. 109 (1998) 2672.